REPORT DOCUMENTATION PAGE

Form Approved OMB NO. 0704-0188

1. REPORT DATE (DD-MM-YYYY)	2. REPORT TYPE	3. DATES COVERED (From - To)
24-08-2015	Book Chapter	-

4. TITLE AND SUBTITLE
Fast Reacting Nano-Composite Energetic Materials: Synthesis and Combustion Characterization

5a. CONTRACT NUMBER
W911NF-14-1-0250

5b. GRANT NUMBER

5c. PROGRAM ELEMENT NUMBER
611102

6. AUTHORS
Keerti Kappagantula, Michelle L. Pantoya

5d. PROJECT NUMBER

5e. TASK NUMBER

5f. WORK UNIT NUMBER

7. PERFORMING ORGANIZATION NAMES AND ADDRESSES
Texas Technical University
Box 41035
349 Admin Bldg
Lubbock, TX 79409 -1035

8. PERFORMING ORGANIZATION REPORT NUMBER

9. SPONSORING/MONITORING AGENCY NAME(S) AND ADDRESS (ES)
U.S. Army Research Office
P.O. Box 12211
Research Triangle Park, NC 27709-2211

10. SPONSOR/MONITOR'S ACRONYM(S)
ARO

11. SPONSOR/MONITOR'S REPORT NUMBER(S)
64880-EG.12

12. DISTRIBUTION AVAILIBILITY STATEMENT
Approved for public release; distribution is unlimited.

13. SUPPLEMENTARY NOTES
The views, opinions and/or findings contained in this report are those of the author(s) and should not contrued as an official Department of the Army position, policy or decision, unless so designated by other documentation.

14. ABSTRACT
Energetic composites are mixtures of solid fuel and oxidizer particles that when combined offer higher calorific output than monomolecular explosives. The composites traditionally deliver energy as diffusion limited reactions and thus their power available from reaction is much smaller than any explosive. Yet, technology has advanced particle synthesis, and nanoparticles have become more readily available. The advent of nanoparticle fuels enables traditionally diffusive controlled reactions to transition towards kinetically dominant reactions. This transition results in faster reacting formulations that show promise of harnessing the power equivalent to a monomolecular

15. SUBJECT TERMS
aluminum combustion; energetic materials; fluorine; reaction kinetics; fluoropolymers; self-assembeled monolayers

16. SECURITY CLASSIFICATION OF:			17. LIMITATION OF ABSTRACT	15. NUMBER OF PAGES	19a. NAME OF RESPONSIBLE PERSON
a. REPORT	b. ABSTRACT	c. THIS PAGE			Michelle Pantoya
UU	UU	UU	UU		19b. TELEPHONE NUMBER 806-742-3563

Report Title

Fast Reacting Nano-Composite Energetic Materials: Synthesis and Combustion Characterization

ABSTRACT

Energetic composites are mixtures of solid fuel and oxidizer particles that when combined offer higher calorific output than monomolecular explosives. The composites traditionally deliver energy as diffusion limited reactions and thus their power available from reaction is much smaller than any explosive. Yet, technology has advanced particle synthesis, and nanoparticles have become more readily available. The advent of nanoparticle fuels enables traditionally diffusive controlled reactions to transition towards kinetically dominant reactions. This transition results in faster reacting formulations that show promise of harnessing the power equivalent to a monomolecular explosive, but packaged as discretely separate fuel and oxidizer composites.

This chapter will focus on developing an understanding of fundamental reaction dynamics associated with particulate media, in general. Once this foundational understanding is established, new strategies for designing aluminum fuel particles toward greater reactivity and thus faster reacting formulations will be presented. In addition to synthesis, several combustion characterization techniques will be examined to quantify combustion performance. All of this information will provide a basis for future research and applications involving aluminum based fuels in any energetic system (i.e., as an additive to liquid propellants or even explosive formulations).

Composite energetic materials with nanoscale aluminum particles play a significant role in nearly every sector of our energy generating economy from industrial to ordnance technologies. Nanoscale aluminum fuel particles hold numerous advantages over their micron scale counterparts. Fluoropolymers have been gaining popularity over the last decade as a favored oxidizer in these composite systems because of their unique ability to react with the passivating alumina shell present over aluminum particles. This chapter investigates the tailorability of energetic composites made of nano aluminum (Al) combined with different fluoropolymers, by incorporating different additives into the reactive material. Diffusion controlled reactions are limited by the proximity (i.e., diffusion distance) of reactant particles. The effect of the proximity of the oxidizer was also investigated by performing flame propagation experiments on molybdenum trioxide (MoO_3) combined with aluminum particles with and without surface functionalized perfluoro tetradecanoic (PFTD) acid. Results showed that the surface functionalization enhanced the burn rate twice that of non-functionalized energetic composite. In order to control the burn velocity by altering their surface functionalizations, three different energetic composites consisting of aluminum particles with and without surface functionalization, combined with molybdenum trioxide was performed. Perfluoro tetradecanoic (PFTD) and perfluoro sebacic (PFS) acids were used to form organic corona around the aluminum nanopartices. Flame propagation studies revealed that energetic composites made of Al functionalized with PFTD (Al-PFTD) displayed burn velocity 86% higher than Al/MoO_3 whereas Al with PFS/MoO_3 are almost half of Al/MoO_3. Results showed that the fluorine content in the acids and their structural differences contribute to difference in burn velocity. The mechanisms controlling reactivity will be discussed such that new approaches to particle synthesis can be developed to further advance energetic composites for the next generation.

Fast Reacting Nano-Composite Energetic Materials: Synthesis and Combustion Characterization

Michelle Pantoya[1] and Keerti Kappagantula[2]

[1]Mechanical Engineering Department, Texas Tech University, Lubbock, TX 79409-1021
[2]Department of Mechanical Engineering, Ohio University, Athens OH 45701 USA

ABSTRACT

Energetic composites are mixtures of solid fuel and oxidizer particles that when combined offer higher calorific output than monomolecular explosives. The composites traditionally deliver energy as diffusion limited reactions and thus their power available from reaction is much smaller than any explosive. Yet, technology has advanced particle synthesis, and nanoparticles have become more readily available. The advent of nanoparticle fuels enables traditionally diffusive controlled reactions to transition towards kinetically dominant reactions. This transition results in faster reacting formulations that show promise of harnessing the power equivalent to a monomolecular explosive, but packaged as discretely separate fuel and oxidizer composites.

This chapter will focus on developing an understanding of fundamental reaction dynamics associated with particulate media, in general. Once this foundational understanding is established, new strategies for designing aluminum fuel particles toward greater reactivity and thus faster reacting formulations will be presented. In addition to synthesis, several combustion characterization techniques will be examined to quantify combustion performance. All of this information will provide a basis for future research and applications involving aluminum based fuels in any energetic system (i.e., as an additive to liquid propellants or even explosive formulations).

Composite energetic materials with nanoscale aluminum particles play a significant role in nearly every sector of our energy generating economy from industrial to ordnance technologies. Nanoscale aluminum fuel particles hold numerous advantages over their

micron scale counterparts. Fluoropolymers have been gaining popularity over the last decade as a favored oxidizer in these composite systems because of their unique ability to react with the passivating alumina shell present over aluminum particles. This chapter investigates the tailorability of energetic composites made of nano aluminum (Al) combined with different fluoropolymers, by incorporating different additives into the reactive material. Diffusion controlled reactions are limited by the proximity (i.e., diffusion distance) of reactant particles. The effect of the proximity of the oxidizer was also investigated by performing flame propagation experiments on molybdenum trioxide (MoO_3) combined with aluminum particles with and without surface functionalized perfluoro tetradecanoic (PFTD) acid. Results showed that the surface functionalization enhanced the burn rate twice that of non-functionalized energetic composite. In order to control the burn velocity by altering their surface functionalizations, three different energetic composites consisting of aluminum particles with and without surface functionalization, combined with molybdenum trioxide was performed. Perfluoro tetradecanoic (PFTD) and perfluoro sebacic (PFS) acids were used to form organic corona around the aluminum nanopartices. Flame propagation studies revealed that energetic composites made of Al functionalized with PFTD (Al-PFTD) displayed burn velocity 86% higher than Al/MoO_3 whereas Al with PFS/MoO_3 are almost half of Al/MoO_3. Results showed that the fluorine content in the acids and their structural differences contribute to difference in burn velocity. The mechanisms controlling reactivity will be discussed such that new approaches to particle synthesis can be developed to further advance energetic composites for the next generation.

1. INTRODUCTION

Combustion can be defined as a rapid chemical reaction that produces heat and light. For composite energetic materials the reacting materials consist of a fuel and an oxidizer. Once the reactive materials come together, if there is enough energy to initiate the reaction, combustion occurs. When one of the reactants (i.e., either fuel or oxidizer) has nanoscale dimensions, the composite is referred to as a nano-composite energetic material. If the energy obtained from combustion is more than necessary to sustain the reaction, energy spreads to the surrounding reactants. As the energy of the surrounding reactants also

reaches a threshold, continued combustion is initiated and energy transfers, thus propagating the combustion (Turns 2012).

For a combustion reaction to be initiated, the participating reactants should possess energy beyond a certain threshold, called *activation energy*, a term coined by Svante Arrhenius. He defined a relationship between activation energy and reaction rate *k(T)* according to equation [1.1]:

$$k(T) = A.exp\left(-\frac{E_a}{RT}\right) \qquad \text{Equation [1.1]}$$

where *A* is the pre-exponential factor, *R* is the gas constant and *T* is the absolute temperature. The activation energy of an exothermic reaction as a function of the reaction path is depicted in figure 1.1. The initiation of a combustion reaction is commonly referred to as ignition. Reactants can be ignited using several approaches such as thermal, mechanical, electrical, shock, optical, chemical or acoustic stimuli. Each method gives rise to unique combustion characteristic depending on the state of the reactants and the heating rate among other factors.

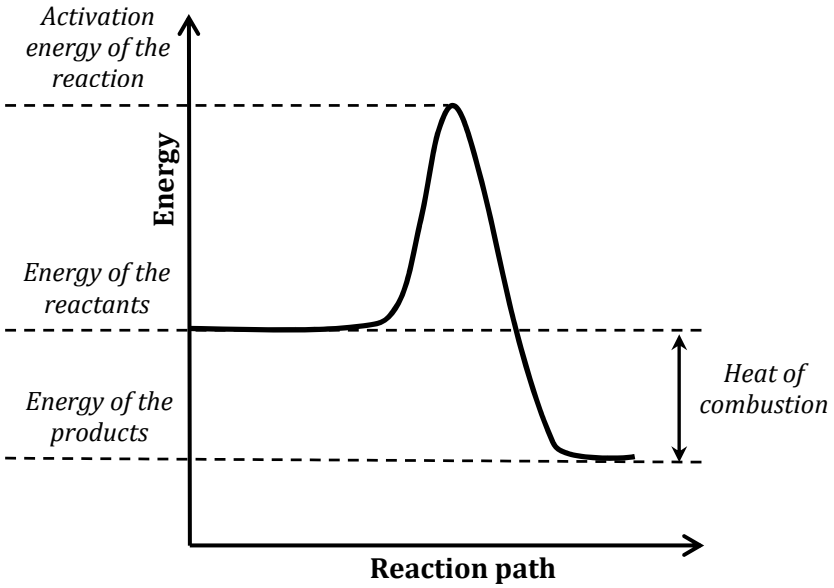

Figure 1.1. Plot showing energy as a function of reaction path during an exothermic combustion reaction.

After reactants are ignited, since combustion is exothermic by nature, the chemical reaction generates enough energy to drive the surrounding reactants to their activation energy and thus, ignition. The cycle of ignition and energy transfer then repeats consequently throughout the reactants and is physically manifested as a flame. A thorough review of the different theories available in literature discussing ignition and propagation in combustion of composites is provided by Farley et al (Farley 2013).

Energetic materials are broadly classified into homogeneous and heterogeneous materials. Homogeneous reactive materials, sometimes referred to as monomolecular energetics or explosives (like TNT, HMX, RDX, PETN, etc.), include fuel (i.e., carbon and hydrogen) and oxidizer (i.e., oxygen, fluorine and nitrogen) bonded within the same molecule. Combustion occurs when the activation energy barrier is reached through external stimuli and the bonds in the homogeneous reactive material are broken. What follows is a very quick release of energy. Since the time scale for energy release is small because the controlling mechanism is bond breaking, the power delivered from these materials is high. However, by the very nature of being monomolecular, they often have an imperfect fuel-oxidizer ratio and thus, low energy density.

Heterogeneous reactive materials, also called energetic composites, consist of physical mixtures of fuel and oxidizer components. The fuels in physical contact with oxidizer undergo combustion at the points of contact. Figure 1.2 shows a particulate composite mixture of magnesium (Mg) fuel combined with manganese oxide (MnO). Rates of reaction are limited by the diffusion of particles and are comparatively lower. But, compared to monomolecular explosives, energy density is very high (i.e., ~ 16,736 J/g for aluminum and molybdenum trioxide ($Al+MoO_3$) compared with 2094 J/g for TNT). Homogeneity of the fuel-oxidizer mixture and the size of the particles become important factors in determining the rate of energy release and therefore the power available from reaction. Energetic composites offer versatility in many parameters to control reactivity including, particle size, formulation, composition, number of reactants, fuel-to-oxidizer ratios, to name a few. In this way, energetic composites may be tailored for specific applications that require increased reliability, controlled reaction rates, tailored sensitivity and hence enable multifunctionality.

Figure 1.2. Scanning Electron Microscopy (SEM) with color mapping to show magnesium particles in red and manganese oxide particles in green.

Conventional energetic composites contain particles ranging in size between 1 to 100 μm. Since classical combustion theory suggests that these reactions are diffusion controlled, decreasing the size of the reactant particles decreases the transport distance and thus enhances the operative mechanism, thereby increasing reaction velocity. Decreasing the particle size from micron to nano scale considerably increases the surface area to volume ratio. A larger ratio will imply decreased diffusion distances between the particles, increased number of contact points between the reactants and subsequently, greater reactivity. Nanoscale energetic composites are thus known to exhibit greater reaction velocities than their micron scale counterparts, although the energy density of the bulk materials remains identical.

Brown et al. decreased the particle size of the Sb/$KMnO_4$ system from 14 to 2 microns and found that the burn rate increased from 2-8 mm/s to 2-28 mm/s (Brown, Taylor and Tribelhom 1998). Shimizu et al. showed that an increased number of contact points between the fuel and oxidizer in the Fe_2O_3/V_2O_5 system increased the reaction rate of the components (Shimizu and Saitou 1990). Aumann et al. examined nano aluminum in the loose powdered media and suggested that aluminum thermite mixtures with an average particle size 20-50 nm reacted almost 1000 times more than conventional thermites, because of the reduced diffusion distance between the individual reactants (Aumann, Skofronick and Martin 1995).

Bockmon et al. showed that when the size of the reactants is reduced from micron to nano scale, reaction velocities increase by up to 1000 times for loosely packed powders (Bockmon, et al. 2005).

Aluminum (Al) has been a preferred fuel in nanoenergetic composites finding extensive use in ordnance and industrial applications, because of its high heat of combustion (~32 kJ/g) (S. H. Fischer 1998). An aluminum oxide (Al_2O_3) or alumina shell of 2-4 nm thickness, forms a barrier between the pure Al core and available oxygen and reduced the spontaneous pyrophoric nature of the fuel, making aluminum particles stable and easy to work with. Figure 1.3 shows TEM images of Al particles, with the alumina shell.

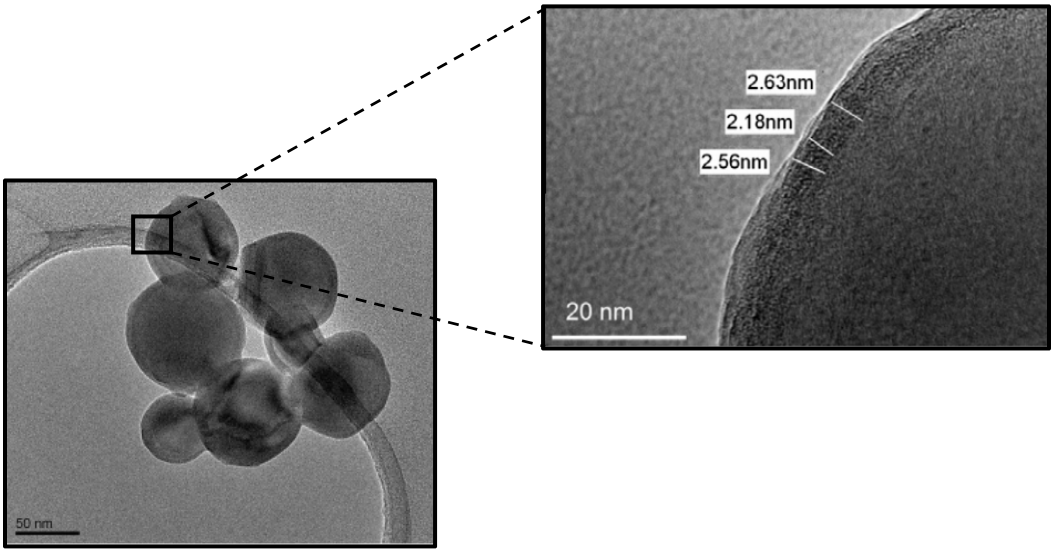

Figure 1.3. TEM images of aluminum nanoparticles with aluminum oxide shell (Gesner, Pantoya and Levitas 2012).

For micron size Al particles, the alumina shell accounts for about 1% of the particle weight. On the other hand, for nanoscale Al particles, depending on the diameter, the Al_2O_3 shell forms 20-45% of the total weight, which is a substantial part of the particle. However, the alumina shell typically does not participate in combustion and acts more like a heat sink. It also forms a barrier between the oxidizer and active Al core, hindering the particle's oxidation. Depending on the size of the Al particles, reaction takes place when the fuel or oxidizer diffuses through the alumina shell. Thus, alumina behaves both as a barrier to Al oxidation and a heat sink at elevated temperatures.

Fluorine (F) is one of the few elements strong enough to react with alumina and the aluminum-fluorine bond is one of the strongest in nature (665 kJ/mol). In fact, fluorine is the most reactive element and is often called a material of extremes (Johns and Stead 2000), because it is the most electronegative. Since it is so reactive, fluorine gas is not commercially used as a reactant. However, fluorine also forms an extremely strong bond with carbon (536 kJ/mol). French chemists, Dumas and Peligot are credited for displaying the stability of the C-F bond (Kirsch 2004). The discovery of polytetrafluoroethylene (PTFE) by Roy Plunkett of Dupont in 1938, when he was experimenting with tetrafluoroethylene (TFE) to create a safe refrigerant, was the beginning of the fluoropolymer era in earnest (McKeen 2006).

Shortly after PTFE was manufactured commercially, the use of fluoropolymers in energetic composites began (Koch, Metal-fluorocarbon pyrolants: III. Development and application of magnesium/teflon/viton (MTV) 2002). Since then, fluropolymers have found widespread use in the energetic community as favored oxidizers and/or reactive binders (Koch, Metal-fluorocarbon pyrolants IV: Thermochemical and combustion behavior od magnesium/teflon/viton (MTV) 2002), (S. Nandagopal 2009). Combinations of PTFE with strong electropositive metals such as Al, magnesium (Mg) and silicon (Si) dominate the literature as examples of PTFE based energetic composites (Yarrington, Son and Foley 2010), (Dreizin 2009), (Pantoya and Dean 2009), (Kappagantula and Pantoya, Experimentally measured themal transport properties of aluminum-polytetrafluoroethylene nanocomposites with graphene and carbon nanotube additives 2012), (Kappagantula, Pantoya and E., Impact ignition of aluminim-teflon based energetic materials impregnated with nano-structured carbon additives n.d.), (Clayton, et al. 2013), (Kettwich, et al. 2014). Fluoropolymers are also known for their thermal stability and chemical resistance which is welcomed in the field of energetics where safety is always a primary concern.

To better understand the oxidizing nature of fluoropolymers and their highly exothermic reaction with electropositive metal, it is helpful to understand the decomposition mechanism of the fluoropolymer into its reactive components. Thermal degradation of PTFE occurs exothermically around 460-610 ^{o}C and depends greatly on the environment. Heating PTFE in air leads to the formation of its monomer, TFE (C_2F_4) and carbonyl fluoride (COF_2).

The monomer, TFE can further decompose into difluorocarbene ($:CF_2$). On the other hand, in vacuum or inert environment, decomposition of PTFE is endothermic, forming TFE and a mixture fluorocarbons, including cyclic fluorocarbons (Koch, Metal-fluorocarbon pyrolants: III. Development and application of magnesium/teflon/viton (MTV) 2002), (Moldoveanu 2005).

The mechanism for the reaction between Al and F is an area of intense focus within the energetics community (Yetter, Risha and Son 2009), (Watson, Pantoya and Levitas 2008), (Dreizin 2009). Osborne et al. investigated the reaction between the alumina shell on Al particles and PTFE and found that an exothermic pre-ignition reaction (PIR) occurs involving the fluorination of Al_2O_3 by PTFE before the oxidation of the active Al core. This was the first time the alumina shell surrounding the aluminum core was found to exothermically contribute to the overall reaction energy. The idea of using alumina as a catalyst bed to excite exothermic reaction that contributes to the overall exothermicity of the reaction was born (D. Osborne 2007)). The first studies exploring this surface reactivity showed that the exothermicity of the PIR was highly dependent on the surface area to volume ratio of the fuel particles (D. Osborne 2007). They also showed the PIR was constant regardless of fuel to oxidizer ratio. Figure 1.4 is a heat flow curve from a differential scanning calorimeter analysis of Al + PTFE for varied fuel to oxidizer ratio. The PIR is constant for fuel lean to fuel rich formulations. The PIR is especially large for nano-aluminum particles because the high surface area to volume ratio promotes more surface exothermic chemistry than micron-scale particles.

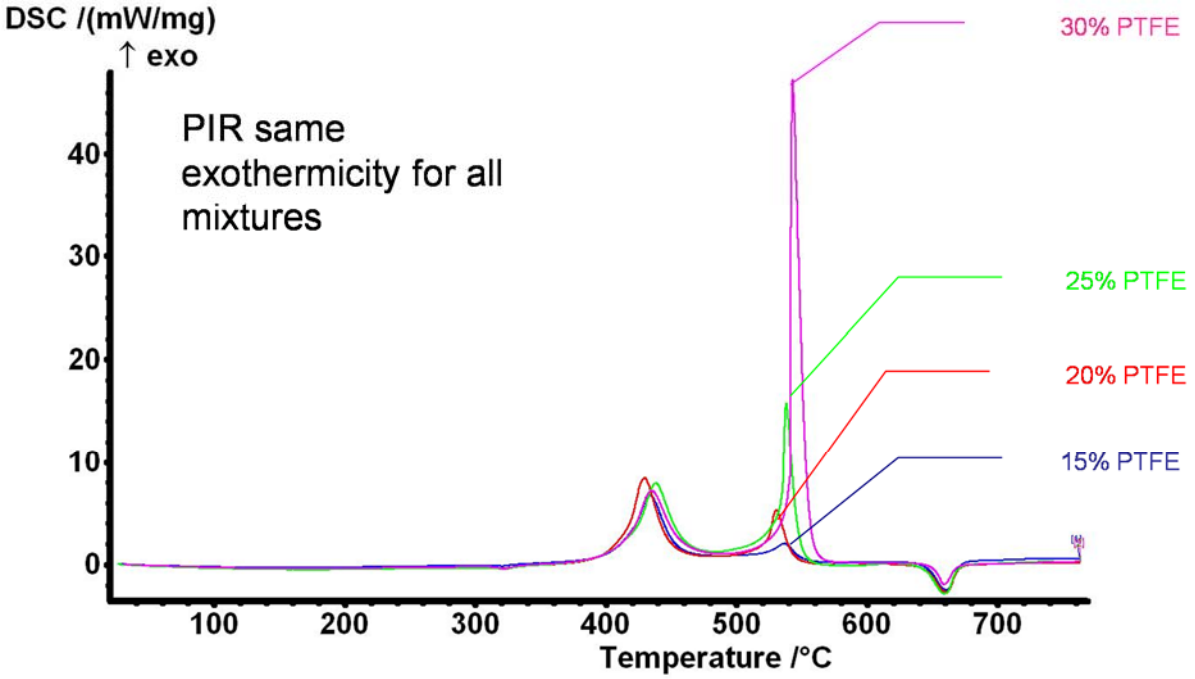

Figure 1.4 Heat flow as a function of temperature in an argon environment for nano particles of Al and PTFE as a function of fuel-to-oxidizer ratio (in terms of PTFE weight percent concentration). Initial exothermic peak is the PIR.

Watson et al. (Watson, Pantoya and Levitas 2008) studied the influence of the gases released during the burning of an energetic composite made of Al, PTFE and molybdenum trioxide (MoO_3). Mixtures of Al/PTFE and Al/PTFE/ MoO_3 were burnt in open and confined set-ups. Results showed that confinement had a dramatic effect on the burn velocities of Al/PTFE, leading to a 200 fold increase. They suggested that without confinement, the gases decomposed from PTFE did not fully react with Al as the products diffused away. Confining the reactants enhanced reaction dynamics, effectively forcing the fluorine from decomposing PTFE to react with the alumina shell surrounding Al particles thereby activating Al oxidation and thus producing higher burn velocities. Table 1 shows the dramatic difference between flame speeds in the open and confined configuration (Watson, Pantoya and Levitas 2008). Surface exothermic reaction kinetics between fluorine from PTFE and the alumina surface may contribute to promoting high flame speeds, especially when coupled with MoO_3.

Table 1. 50 nm Al particles combined with polytetrafluoroethylene (PTFE) and/or molybdenum trioxide (MoO_3). See (Watson, Pantoya and Levitas 2008)**.**

Wt. % Al	Burn velocity (m/s)					
	Open Burning Configuration			Confined Burning Configuration		
	Al/PTFE	**Al/MoO_3/PTFE**	**Al/MoO_3**	**Al/PTFE**	**Al/MoO_3/PTFE**	**Al/MoO_3**
10	0.00	0.00	2	0.00	0.00	88
20	0.14	11	23	0.01	351	557
30	1.6	356	435	299	690	901
40	3.2	410	456	837	957	960
50	4.2	230	201	752	816	756
60	2.6	76	31	562	272	393
70	2.3	9	3	386	72	160
80	1.3	1	0.8	79	8	0.00
90	0.00	0.30	0.06	0.00	0.00	0.00

Yarrington et al. studied the combustion characteristics of loose powder and pressed pellets of mixtures of Al, PTFE (trade name Teflon®) and a binder, poly(hexafluoropropylene-co-vinylidene fluoride) (HFP-VF) (trade name Viton®), known as AlTV. Chemical equilibrium codes were used to identify the fuel-to-oxidizer ratios, dominant products, reaction temperatures and pressures. Burn velocities of the pellets increased with increasing Al content and optimized speeds were obtained at 58% wt., far beyond the stoichiometric condition of 28% wt. observed during the flame tube studies. The researchers suggested that the AlTV reactions occur in both condensed and gas phases.

For high speed reactions, PTFE dominates the energetic composite research as the most common source of fluorine that produces flame speeds on the order of 1000 m/s. But, there are other fluoropolymers experimented upon. Graphitic fluoride $(\text{-CF-})_n$ has been shown to outperform PTFE as an oxidizer in energetic formulations, yielding higher combustion temperatures (Koch, Metal-fluorocarbon pyrolants: V. Theoretical evaluation of the combustion performance of metal-fluorocarbon pyrolants based on strained fluorocarbons 2004). Cudzilo et al. (Cudzilo, et al. 2007) reported highly exothermic and self-sustaining reactions between $(\text{-CF-})_n$ and several fuel particles including silicon (Si) and Al-

Si alloys. They showed that exfoliated graphite is the dominant product produced despite the fuel used.

Iacono et al. explored the use of perfluoropolyethers (PFPE), fluorinated polyurethanes and copolymers of the two, as fluorinated matrices for the preparation of energetic composites with Al fuels in different structural forms like pellets, fibers and cylindrical "pucks" (Fantasia, et al. 2011), (Danielson, et al. 2013), (Pierson, et al. 2011) (Clayton, et al. 2013). As opposed to PTFE, PFPE is a liquid, paste-like oligomer that wets the surface of Al particles, effectively coating them.

Fluoropolymers have been used as binders in energetic composites. HFP-VF has been applied as a reactive binder in the place of hydrocarbons such as hydroxyl terminated polybutadiene (HTPB). Nandagopal et al. (S. Nandagopal 2009) coated ammonium perchlorate (AP) particles with HFP-VF in propellant formulations and showed that Al/HTPB/AP had increased thermal stability compared to control energetic composites without the HFP-VF binder, thereby providing a safer and easier to handle solid rocket propellant.

This chapter will focus on exploring synthesis approaches to activating Al fuel particles in order to produce fast reacting formulations. The goal is to improve Al reactivity by exploiting exothermic surface chemistry inherent in the alumina shell. At one time, the alumina shell was considered dead weight in the reaction: (1) a barrier to Al oxidation, limiting Al reactivity; and, (2) a heat sink during the production of liberated chemical energy. However, alumina is an active catalyst and exploiting catalytic reactions on the alumina surface to effectively enhance Al oxidation towards production of fast reacting mixtures is an important avenue for future energetic materials development.

2. EFFECT OF FUEL AND OXIDIZER PROXIMITY ON COMBUSTION

Although decrease in the reactant size enhances reactivity, there are several problems associated with nanoscale reactants. The higher surface energy of the nanoparticles leads to greater particle aggregation (in order to minimize the free energy of the system) which makes homogenizing the composite very difficult (J. Brege 2009). Another

issue associated with the high surface area of the nanoparticles is the increased amount of viscosity when the nanoparticles are introduced into a solvent during composite preparation, which can lead to unwanted friction generation during particle mixing and increased composite agglomeration (R. J. Jouet 2005). Apart from these, however, one of the biggest problems is excessive oxidation of the fuel particle (Al) before combustion (R. Brewer 2006). In general nano Al particles have a passivating alumina (Al_2O_3) shell with an average thickness of 1.7 to 6.0 nm (D. Pesiri 2004), which accounts for almost 25 to 40 % of the entire volume, depending on the particle size. Although the oxide layer is an inert coating, prolonged exposure to air or moisture will further oxidize the Al particle, thus depleting the active Al content over time, thereby aging the fuel.

One technique to counter these problems is chemical functionalization of the nanoparticle surface. In general, surface functionalization refers to the process of encompassing the nanoparticles in an organic corona. Because the Al particles have a surrounding Al_2O_3 shell, the material used for surface functionalization should be capable of interacting either physically or chemically with the alumina shell. Under standard atmospheric conditions, the Al_2O_3 shell can become partially hydroxylated (K. Wefers 1988), providing an additional route for surface functionalization. Ample literature is available about the chemical functionalization of Al_2O_3 oxide on bulk Al particles using the condensation of carboxylic acids to surface bound hydroxyls in order to form self assembled monolayers (SAMs) (K. Oberg 2001), (M. Lee 2007), (M.E. Karaman 2001). Successful functionalization of alumina with silanes (M. Abela 1998), phosphoric acids (I. Liakosa 2008) and hydroxamix acids (J. Folkers 1995) has been demonstrated. Research shows that the physical properties of these nanoparticles are functions of the physical and chemical compositions of the surface corona to a great extent (C. Crouse 2010), (D. Weibel 2010).

Developing new Al based nanocomposite systems that possess energetic properties tailored for a desired application often requires the use of very large particle loadings. This has been achieved by using perfluoroalkyl carboxylic acids (R. J. Jouet 2005), silanes (S. Valliappan 2005) and glycols (R. Thiruvengadathan 2011) among others. It was seen that the combustion performance of such Al nanocomposites was affected by the presence of

functional groups on these particles; combustion velocities of such nanocomposites decreased with the presence of hydroxyl groups (B. Dickiki 2009).

Surface functionalization of Al nanoparticles without the alumina shell was achieved too (R. J. Jouet 2005). However, flame propagation studies of energetic nanocomposites made with such Al particles showed that their burn velocity was very low compared to energetic nanocomposites consisting of Al with alumina shell and no surface functionalization (B. Dickiki 2009). In addition, the method of preparation of such perfluoroalkyl carboxylic acid coated Al particles without the alumina shell was deemed unfit for mass production because partial fluorine passivation led to an extremely pyrophoric material. Perfluoroalkyl acids are particularly interesting as coatings over Al particles because using fluorinated compounds offers an added increase in energy content of the system during combustion because fluorine can act as an oxidizer for aluminum. In fact, the formation of AlF_3 releases 55.67 KJ/g of Al, which is a significant increase over the formation of Al_2O_3 (30.96 KJ/g) (CRC Handbook of Chemistry and Physics 1991). In an effort to capitalize on this potential, nano Al particles with an Al_2O_3 shell were coated with perfluoroalkyl tetradecanoic (PFTD) acid in an effort to improve their reaction kinetics (J. Horn 2011).

Aluminum particles with and without surface functionalization were synthesized and combined with molybdenum trioxide and their flame propagation characteristics were measured and analyzed. Potential factors relating the burn velocity of the energetic composites and their chemical makeup are identified in order to improve the understanding of fast reacting energetic nanocomposite systems (Kappagantula, Pantoya and Horn, Effect of surface coatings on aluminum fuel particles toward nanocomposite combustion 2013).

2.1. Materials and sample preparation

Aluminum particles with 80 nm average particle diameter were used as fuels in this study. All the Al particles were encapsulated in an alumina (Al_2O_3) passivation shell with an average thickness of 2.7 nm with an active Al content of 86% by volume. Surface functionalization of the Al results in a 5 nm thick layer (35% by weight) of perfluorotetradecanoic acid (PFTD) bonded to the Al-Al_2O_3 core-shell particle. The detailed preparation method for the acid coated Al particles may be obtained elsewhere (J. Horn

2011). The second type of Al particles had an alumina passivation shell without acid coating and will be referred to as Al. Molybdenum trioxide (MoO_3) is used as the principal oxidizer and has a flake like morpohology with 44 nm average flake thickness.

The three different composites, identified as Al/MoO_3/PFTD, Al-PFTD/MoO_3, and Al/MoO_3, were prepared for the flame propagation experiments. The Al/MoO_3/PFTD is a physical mixture of discretely separated powders of Al, PFTD powder and MoO_3. In contrast, the Al-PFTD/MoO_3 includes MoO_3 and Al particles coated with PFTD chains. This sample has Al chemically bonded to PFTD. The Al/MoO_3 consists of Al and MoO_3 alone. The redox reactions between Al, the PFTD functionalization and MoO_3 are complex; hence, the reactant concentrations are expressed in terms of mass percentages and not in terms of equivalence ratio. Dikici et al. (B. Dickiki 2009) showed that similar Al-PFTD/MoO_3 combinations with 70.6% by mass MoO_3 have the highest burn velocity and the same Al-PFTD/MoO_3 ratio was adopted here. Since the Al-PFTD particles had 35% by mass of PFTD, the PFTD content accounted for 10.36% of the total Al-PFTD/MoO_3. This implied that the active Al and the Al_2O_3 content in Al-PFTD accounted for 19.06% of the total composite mass. The same mass percentages were assumed for preparing the Al/MoO_3/PFTD composite too in order to keep the chemistry of the reaction constant and vary only the proximity of the PFTD to the Al in order to study its effects on the burn velocity of the composites. The mass percentages of fuel and oxidizers present in the three different composites prepared are given in Table 2.1.

Table 2.1. Fuel and oxidizer reactants, along with their masses in the composites prepared.

Sample name	Fuel	Ox 1	Ox 2	Wt. % Reactants		
				Fuel	Ox 1	Ox 2
Al/MoO_3/PFTD	Al	PFTD powder	MoO_3	19.04	10.36	70.6
Al-PFTD/MoO_3	Al-PFTD	PFTD coating	MoO_3	19.04	10.36	70.6
Al/MoO_3	Al	MoO_3	-	21.24	78.76	-

Measured quantities of reactants required for preparing each composite were suspended in hexanes. The suspension was then sonicated using a Misonix Sonic wand for 120 seconds in 10 second intervals to break agglomerates and improve homogeneity of the

composite. The hexanes suspension was transferred to a Pyrex dish and heated to a temperature of 45^{o}C to facilitate the evaporation of hexane. Once the powder mixture dried, it was reclaimed for further experimentation. This is a standard procedure for combining solid particle reactants.

2.2. Flame propagation experiments

The prepared composites were subjected to flame propagation experiments. A schematic of the experimental set up is shown in figure 2.1. It consists of a quartz tube, 110 mm long, with an inner diameter of 3 mm and an outer diameter of 8 mm. Each composite was loaded into the quartz tube and placed on a vibrating block for 5 seconds to reduce local density gradients. Each tube contained approximately 470 ± 10 mg of composite resulting in a loose powder fill estimated to be 7% of the theoretical maximum density. Once prepared, the tube was placed in a steel combustion chamber with viewing ports for diagnostics. Three quartz tubes were prepared for each composite allowing for an estimate of the repeatability and uncertainty in the measurement.

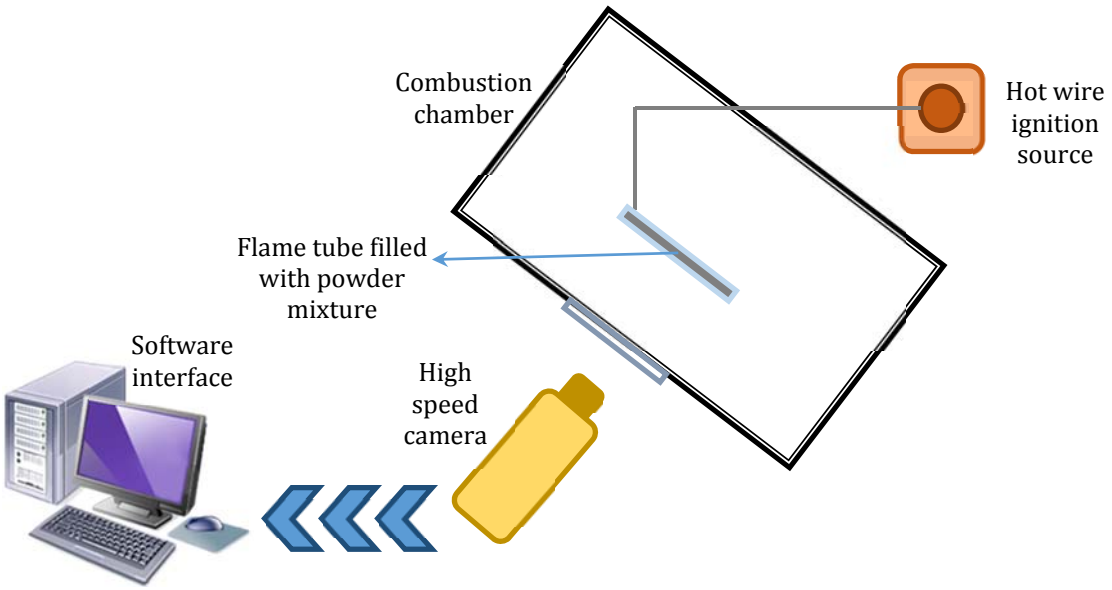

Figure 2.1. Schematic illustrating camera position relative for powder filled flame tube and ignition source.

Ignition was achieved via thermal stimulus provided by a Nichrome wire connected to an external voltage supply. A Phantom v7 (Vision Research, Inc., Wayne, NJ) with a Nikon AF Nikkor 52mm 1:2.8 lens was used to record ignition and flame propagation. The camera

captured images of the reacting composite, perpendicular to the direction of flame propagation, at a speed of 160,000 frames per second, with a resolution of 256 by 128 pixels. Vision Research software was used to post-process the recorded photographic data. When a reference length is established, the software determines speed based on a distance between sequential time frames. Using a "find-edge" image filter that identifies preset variations in pixel intensity, the flame front location (which is identified as the region of the flame with the maximum radiance) is identified and marked for speed measurements. Figure 2.2 shows representative sequential images from high speed imaging of flame propagation through this tube apparatus filled with powder energetic composite.

Figure 2.2 Sequential images of the flame propagating along the tube

2.3. Results

Figure 2.3 shows a representative plot for the distance traversed by the flame front as a function of time. The initial portion of the curve shows unsteadiness as the flame progresses down the quartz tube. Flame speed is measured when propagation attains steady state behavior seen in the latter portion of the tube represented by linearity in the distance versus time plot. The slope of the linear region represents burn velocity.

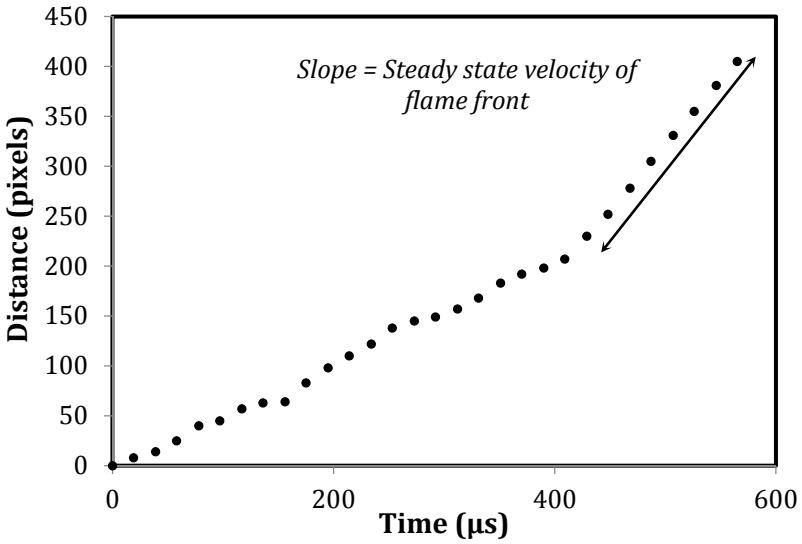

Figure 2.3. Distance travelled by the flame front in the burn tube for Al/MoO_3 composite as a function of time.

The steady state burn velocities are compared in figure 2.4 with bars representing standard deviations. The burn velocity of the acid-coated aluminum (Al-PFTD/MoO_3) is 366% faster than the physical mixture of aluminum and perfluorotetradecanoic acid (Al/MoO_3/PFTD). The burn velocity of the composite with the acid-coated aluminum, Al-PFTD/MoO_3, is almost double that of non-treated nano-aluminum composite, Al/MoO_3. Interestingly, the composite containing the surface functionalized Al, Al-PFTD/MoO_3, had the highest burn velocity in the study while the physically mixed composite, Al/MoO_3/PFTD, had the lowest burn velocity.

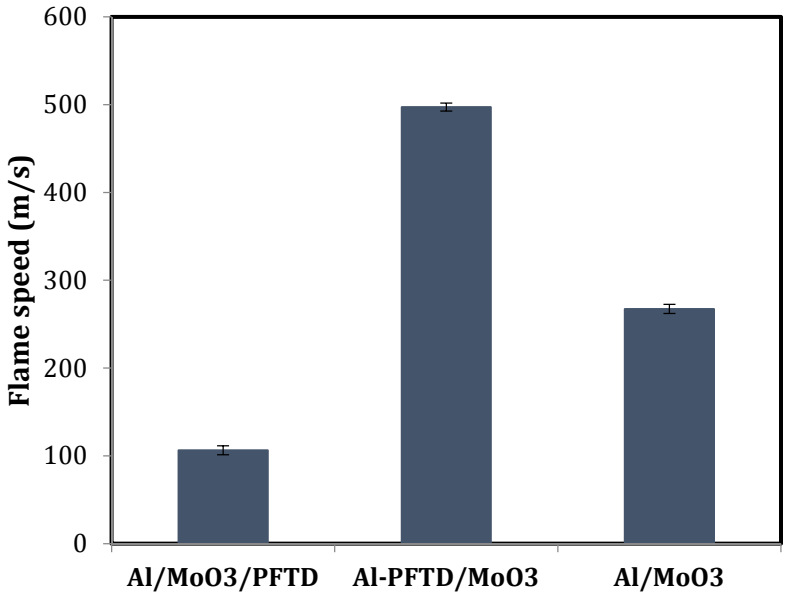

Figure 2.4. Burn velocity of Al/MoO_3/PFTD, Al-PFTD/MoO_3 and Al/MoO_3 with uncertainty measurements.

The increase in the burn velocity of Al-PFTD/MoO_3 may be attributed to the bonding of the oxidizing PFTD to the Al fuel. During the combustion of the acid-coated aluminum, the reaction is hypothesized to progress in two distinct stages. In *Stage 1*, the PFTD chains on the surface of the Al fuel particles react with the Al_2O_3 shell to form AlF_3. Fluorination of the alumina shell is identified as a rate determining step for Al reactions with fluoropolymers (D. Osborne 2007). This interaction makes the Al core readily available for further reactions. The proximity of the PFTD chains in the surface functionalized Al enhances the rate of the fluorination reaction when compared to the unbonded PFTD. Subsequently, in *Stage 2*, the aluminum core undergoes rapid oxidization by the fluorine from the PFTD, MoO_3 and air.

In the case of Al/MoO_3/PFTD composite, the PFTD particles are not bonded to the Al nanoparticle. The diffusion distance between Al and PFTD particles is therefore greater and the fluorination reaction may take longer. As a result, the burn velocity of Al/MoO_3/PFTD is significantly less than Al-PFTD/MoO_3.

The burn velocity of the physically mixed composite, Al/MoO_3/PFTD is lower than the simple Al/MoO_3 composite. In the case of Al/MoO_3/PFTD, there are two competing

reactions progressing during combustion: Al reacting with PFTD and Al reacting with MoO_3. The primary oxidizing component of PFTD is fluorine which reacts with Al_2O_3 and Al. This reaction is similar to Al reacting with polytetrafluoroethylene (PTFE) since the PFTD chains resemble PTFE polymer chains after their initial decarboxylation during reaction. PFTD may start reacting with Al before the MoO_3 does due to its proximity to the Al. Watson *et* al. (Watson, Pantoya and Levitas 2008) showed that the burn velocity of Al with PTFE is lower than with MoO_3. They also showed that the burn velocity of Al with PTFE and MoO_3 combined is lower than Al/MoO_3. Similar trends are mirrored in the results from the current study. Fluorine separation from PFTD may be the rate determining step to reaction with Al and decrease Al's availability to react with MoO_3, making the Al-PFTD the primary reaction. If the slower reaction becomes the primary reaction, then the burn velocity of the entire ternary composite would be less than that of the binary composite, Al/MoO_3. Similar results were observed by Prentice *et* al. (Prentice, Pantoya and Clapsaddle 2005) when they performed flame propagation studies with Al mixed with varying compositions of silicon dioxide (SiO_2) and iron oxide (Fe_2O_3). They showed that Al/SiO_2 had the lowest burn velocity and Al/Fe_2O_3 had the highest, whereas the burn velocities of all composites with increasing percentages of SiO_2 added to Al/Fe_2O_3 had correspondingly decreasing burn velocity. Prentice *et* al. (Prentice, Pantoya and Clapsaddle 2005) showed that for ternary composites, competing reactions with Al tend reduce the burn velocity over the highest binary reaction burn velocity when the mixtures are physically mixed and diffusion limited.

3. TUNING COMBUSTION PERFORMANCE OF ENERGETIC NANOCOMPOSITE THROUGH SURFACE FUNCTIONALIZATION OF THE FUELS

Flame propagation studies of energetic composites made of PFTD functionalized and non-functionalized Al nanoparticles (Al-PFTD and Al, respectively) combined with molybdenum trioxide (MoO_3) demonstrated that the PFTD actively participates in the reaction and contributes to the enhanced flame speed of Al-PFTD/ MoO_3 compared to Al/ MoO_3. However, functionalizing Al particles with PFTD only leads to increased burn velocity. The greater goal is on achieving process control and tailorability of Al particles by studying the flame propagation of Al nanoparticles functionalized with perfluoro carboxylic acids

such that the burn velocity of the corresponding energetic composite will decrease. Thermites are ideal energetic composites because of their tailorability based on manipulating reactant properties. To this effect, a shorter, more sterically hindered organic acid, perfluoro sebacic acid (PFS) was used to functionalize Al nanoparticles according to the procedure in reference in (J. Horn 2011). Experiments were performed to study the thermoequilibrium and non-equilibrium combustion behaviors, using differential scanning calorimetry amd flame propagation experiments. Activation energy (E_a) and burn velocity of the energetic composites was evaluated and the relationship between the structure of the acid coating and the combustion behaviors were investigated (Kappagantula, Farley, et al. 2012).

3.1. Material Synthesis

Three different types of Al with 80 nm average particle diameter were used as fuels. All the Al particles were encapsulated in an alumina (Al_2O_3) passivation shell with an average thickness of 2.7 nm. Al-PFTD particles had a 5 nm thick layer of PFTD over the Al_2O_3 shell. Similarly, particles referred to as Al-PFS hence forth, had a 5 nm thick layer of PFS over the Al_2O_3 shell. It is noted that these acids bond to the alumina shell through the surface hydroxylation. The third type of Al particles had an alumina passivation shell without any acid coating and will be referred to as Al. The structures of PFTD and PFSs are shown in figure 3.1.

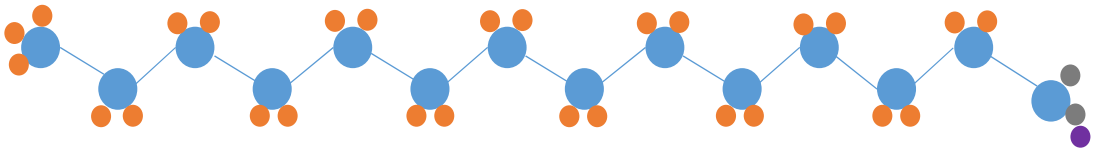

Perfluoro tetradecanoic acid (PFTD)

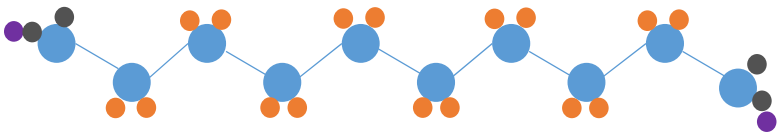

Perfluoro sebacic acid (PFS)

Carbon *Fluorine* *Oxygen* *Hydrogen*

Figure 3.1. Schematic representation of the chemical structure of the PFTD and PFSs, respectively.

The Al nanoparticles used throughout this study were procured from Nova Centrix Corp. Austin, TX, USA. These Al particles were coated with PFTD to obtain Al-PFTD and with PFS to obtain Al-PFS, respectively in slurry of diethyl ether. The powder product was washed three times in diethyl ether to remove any acid that was not bonded to the alumina shell. The end result was Al particles with a perfluoroalkyl acid self-assembled monolayer surrounding the Al_2O_3 shell. The detailed preparation method for these acid coated Al particles may be obtained elsewhere (J. Horn 2011). It was proposed that the perfluoroalkyl acids, PFTD and PFS, bond to the alumina through the carboxylic functional group (R. J. Jouet 2005). The oxidizer comprised of MoO_3 procured from Mach I, USA. The MoO_3 particles have an average thickness of 44 nm with rectangular plate-like morphology, whereas the Al particles are all spherical.

For preparing the energetic composites, requisite amounts of Al fuel (with and without SAMs) and MoO_3 oxidizer were measured and suspended in hexanes. The suspension was then sonicated as described in Section 2.1 following standard mixing procedures for reactive powder preparation. Three energetic composites were prepared corresponding to the three different Al fuels.

3.2. Flame Propagation Experiments

Flame propagation experiments were conducted using the three energetic composites to determine the burn velocity. The flame tube apparatus was used and reported extensively in flame propagation experiments (B. S. Bockmon 2005), (C. Yarrington 2011), (M. Weismiller 2011), (B. Dickiki 2009), (Kappagantula, Clark, et al. 2011). Each energetic composite was loaded into the tube and placed on a vibrating block for 5 seconds to reduce local density gradients. Each tube contained about 468 ± 10 mg of energetic composite resulting in a loose powder fill estimated to be 7% of the theoretical maximum density. Once prepared, the tube was placed in a steel combustion chamber and the experimental setup is schematically represented in figure 2.2. In these experiments, the camera captured images of the reacting composite, perpendicular to the direction of flame propagation, at a speed of

160,000 frames per second, with a resolution of 256 by 128 pixels. The Vision Research software was used to post-process the recorded photographic data.

3.3. Thermal Equilibrium Experiments

Activation energy was found using a thermo equilibrium isoconversion method. Samples of approximately 6 mg were loaded into a Neztsch STA 409 differential scanning calorimeter (DSC) and thermogravimetric analyzer (TGA) and heated to 1273K at 2, 5, or 10 K/min in a 1:3 (by volume) oxygen-argon environment. Within the DSC/TGA, the sample crucible is compared to an empty reference crucible in order to obtain the net energy and mass change. Also, the sample carrier was mounted on a microscale (i.e. TGA) allowing for mass change measurements that relay phase change (i.e. gas production) information as a function of equilibrium temperature. The slope of the DSC curve changes when the reaction within the DSC/TGA produces enough energy to become noticeable within the natural noise of the machine. The area under the DSC curve corresponds with the net exothermic behavior. The activation energies were then calculated using equation (3.1) from the Type B-1.95 peak method as described by M.J. Starink (Starnik 2004).

$$\frac{B}{T_p^{1.95}} = A \exp\left(-\frac{E_a}{RT_p}\right) \tag{3.1}$$

In equation (3.1), B is the heating rate, A is the pre-exponential factor, E_a is the activation energy, R is the universal gas constant and T_p is the temperature at the exothermic peak of the reaction. Reaction rate is approximated by$B/T_p^{1.95}$. Taking the natural log yields equation (3.2).

$$ln\left(\frac{B}{T_p^{1.95}}\right) = -\frac{E_a}{RT_p} + \ln A \tag{3.2}$$

By plotting $\ln(B/T_p^{1.95})$ as a function of $(1/RT_p)$ for the different heating rates, E_a (kJ/mol) can be found as the slope of the trend line.

3.4. Results of Flame Speeds

The activation energy for these samples as well as their burn velocity is shown in Table 3.1. The burn velocity of Al-PFTD/MoO_3 is 86% faster than the burn velocity of Al/MoO_3, whereas the burn velocity of Al-PFS/MoO_3 is almost half of Al/MoO_3.

Table 3.1. Burn velocity and activation energy results.

Energetic Composite	Activation Energy E_a (kJ/mol)	Average Flame Speed (m/s)
Al/MoO_3	252	267
Al-PFTD/MoO_3	185	497
Al-PFS/MoO_3	553	138

Figures 3.2A, B and C show the DSC/TGA plots of the three energetic composites as a function of temperature at three different heating rates: 2, 5 and 10 K/min.

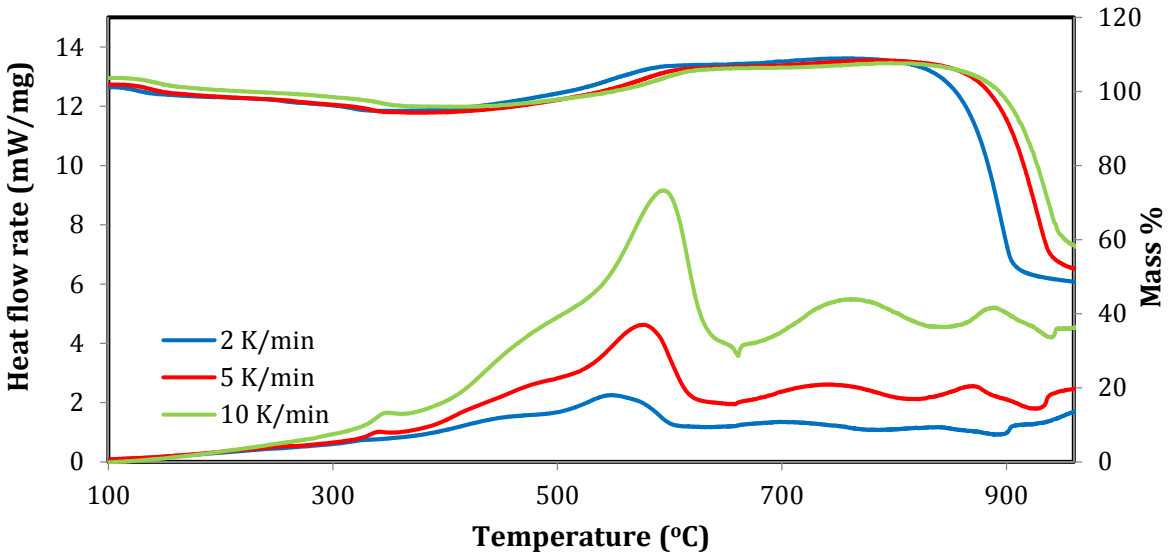

Figure 3.2A. DSC (three plots on the bottom)/TGA three plots on the top) of Al-PFTD/MoO_3 reaction at different heating rates.

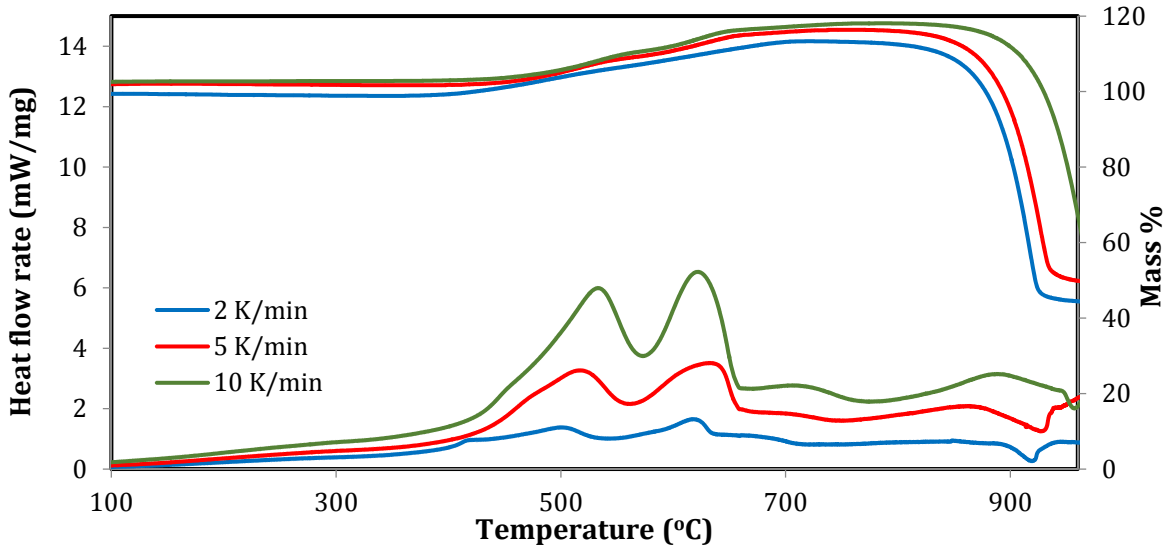

Figure 3.2B. DSC (three plots on the bottom)/TGA (three plots on the top) of Al/MoO_3 reaction at different heating rates.

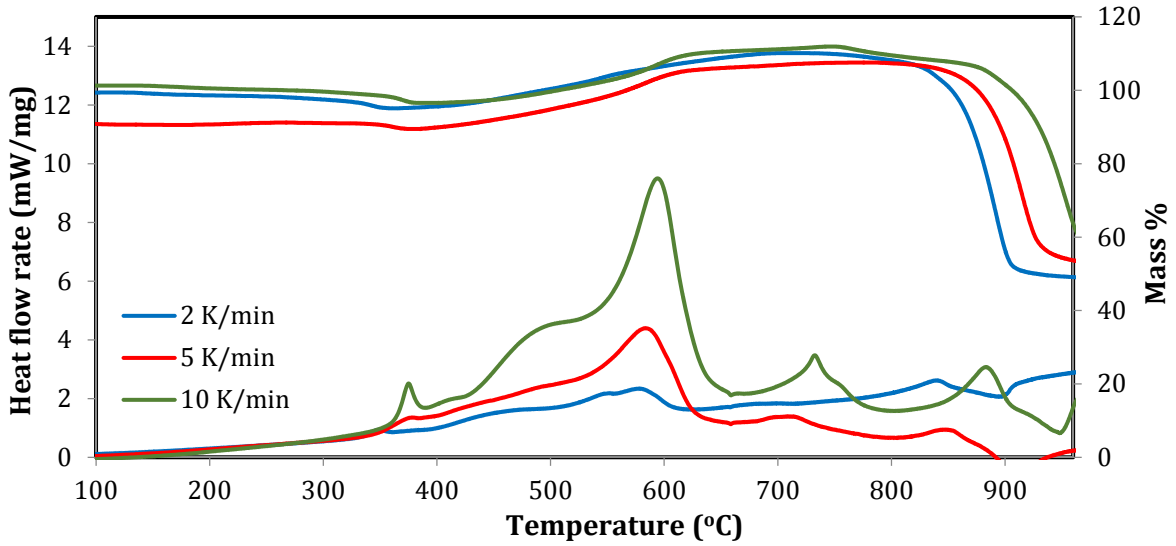

Figure 3.2C. Heat Flow from DSC (three plots on the bottom) and mass loss from TGA (three plots on the top) of Al-PFS/MoO_3 reaction at different heating rates of 2, 5, 10 Kelvin per minute.

Al-PFTD/MoO_3 and Al-PFS/MoO_3 reactions show a smaller exotherm before the bigger one whereas the same is not seen in the Al/MoO_3 reaction plot. On the other hand, the Al/MoO_3 plot shows a two stage exotherm signifying two reactions occurring at two different temperatures. Also, two small endotherms are to be noted on the DSC plots of the energetic composites with acid coated fuels at about 650-660 °C. This temperature corresponds to the

melting point of Al, which might mean that the endotherm may represent the melting of some excess Al left over after it reacts with the MoO_3 present.

Such an endotherm is not present in the Al/MoO_3 DSC plots; there is, however, a second endotherm present in the Al/MoO_3 plot. It may be concluded that the first peak corresponds to the oxidation of Al with MoO_3 particles which is known to occur at around 540 ^oC (J. H. Bae 2010). In order to understand the second peak of the heat curve, a DSC run of the same energetic composite was performed with the identical sample size and heating rate in an exclusively argon (Ar) environment. The resultant heat curve is shown in figure 3.3.

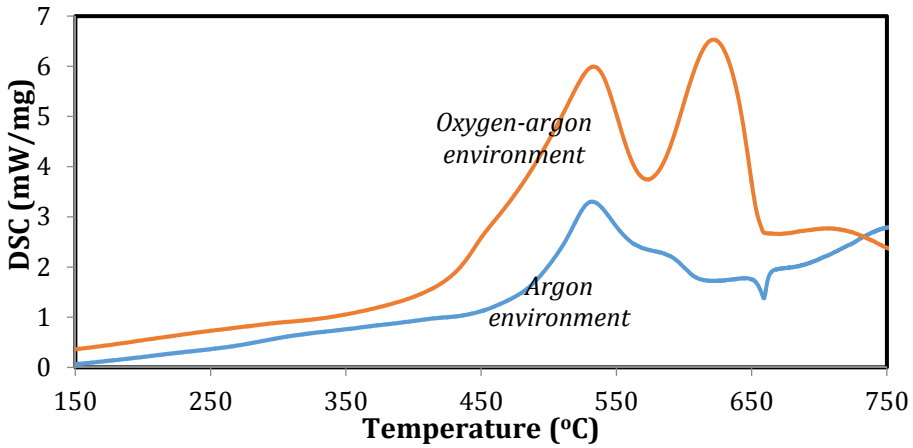

Figure 3.3. Heat flow curve of Al/MoO_3 energetic composite as a function of temperature for a constant 10 K/min heating rate.

The Al/MoO_3 combustion in an Ar environment shows an endothermic dip at about 660 ^oC, (corresponding to unburned Al melting). Comparing this to the heat curve initially observed for Al/MoO_3 (figure 3.3) combustion in an oxygen-argon environment, it may be seen that the second exothermic peak corresponds with the Al melt endotherm. In an entirely argon environment, the only oxidizer available during the reaction would be MoO_3. Once all the MoO_3 is used by the Al fuel present in the redox reaction, any leftover Al particles cannot react with any other oxidizer and hence melt when heated further. On the other hand, in a 1:3 (by volume) oxygen-argon environment, the Al particles have two oxidizers to react with: the MoO_3 mixed in the energetic composite and the oxygen in the reaction environment. Therefore, any Al left behind after the entire amount of MoO_3 is consumed in the redox reaction may be oxidized in the oxygen environment on further heating. This oxidation of Al

by oxygen will result in an exotherm. Therefore, it may be concluded that the second exothermic peak in the heat curve of Al/MoO_3 is due to the unburned Al particles being oxidized by oxygen in the reaction environment. For better comparison, the DSC plots of all the energetic composites for a constant 10 K/min heating rate are provided together in figure 3.4.

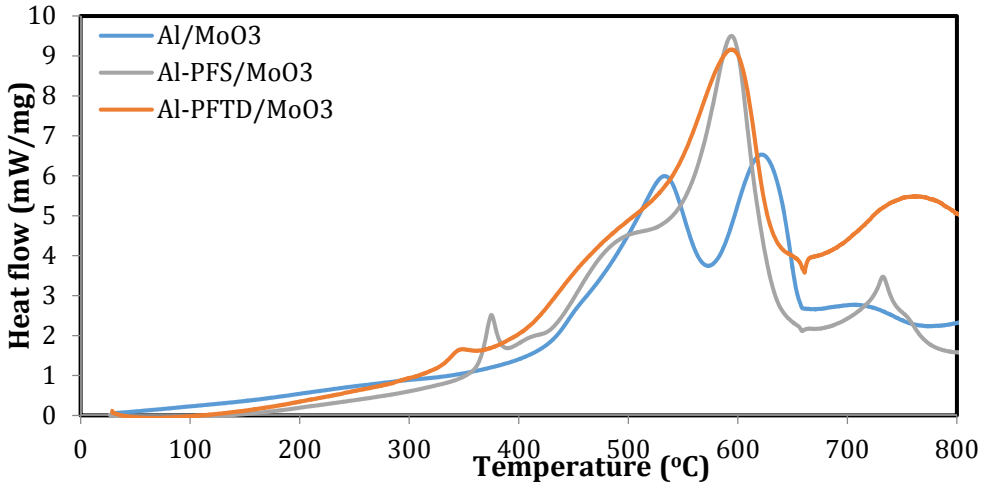

Figure 3.4. DSC curve of each energetic composite as a function of temperature for a constant 10 K/min heating rate.

Figure 3.4 shows that the first exotherm on DSC plot of Al-PFTD/MoO_3 occurs at a lower temperature than the first exotherm on the Al-PFS/MoO_3 plot. The analysis in figure 3.4 is extended to lower heating rates in order to measure the isoconversion temperature corresponding to a continuous transition. Using the values for peak temperature at various heating rates (i.e., 2, 5, and 10 K/min), the ln $(B/T_p^{1.95})$ as a function of $(1/RT_p)$ for each energetic composite was plotted and results are shown in figure 3.5.

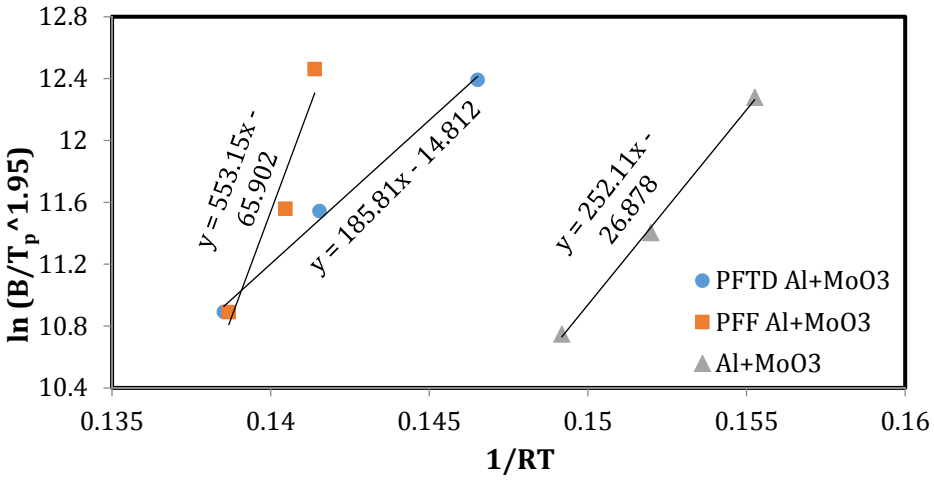

Figure 3.5. Trend lines showing the activation energy of the energetic composite compositions.

The slopes of the trend lines in figure 3.5 are the activation energies (E_a) of the compositions reported in Table 3.1 and shows that the E_a of Al/MoO_3 is 252 kJ/mol, corresponding to the E_a values of the energetic composite as found in literature (J. Sun 2006), (D. Stamatis 2011). The interesting point to note is that the activation energy trend is opposite to that of the burn velocity values, i.e., compositions with low burn velocity have high E_a and vice versa. Since all the parameters like flame tube diameter, length, Al and MoO_3 concentration, TMD and stimulus voltage were maintained constant for all the tests, the contributing factor for the difference in the burn velocity may be the chemical composition and kinetics of the acid shell.

Osborne and Pantoya (D. Osborne 2007) showed that when Al reacts with polytetrafluoroethylene (PTFE), the fluorine reacts with the Al_2O_3 shell at elevated temperatures leading to the formation of aluminum fluoride (AlF_3). This interaction occurs during a pre-ignition reaction (PIR) around 400 ^oC. They postulated that the formation of AlF_3 serves to degrade Al_2O_3 leaving the Al core exposed for further reaction. The acid coatings used here contain a large percentage of fluorine in their alkyl chains terminating in carboxylic groups as illustrated in figure 3.1. PFTD contains 72 % fluorine by weight whereas PFS has 62% fluorine be weight. At elevated temperatures, the fluorine radicals from the acid coating may react with Al_2O_3 (similar to fluorine radicals from PTFE molecules) degrading the alumina shell and exposing the Al core for further oxidation. This can be seen in figure

3.4 when comparing the heat flow curves for the two acid coated energetic composites. Al-PFTD/MoO_3 exhibits a PIR onset at 320 ^oC and peak at 342 ^oC while the Al-PFS/MoO_3 exhibits a PIR onset at 350 ^oC and peak at 374 ^oC. After the PIR in figures 3.3A and 3.3C, the heat flow curves appear similar and there is no further indication of discrepancies in the equilibrium kinetics that account for the differences in burn velocity seen in Table 3.1 (86% increase over Al/MoO_3 in case of Al-PFTD/MoO_3 and 48% decrease in case of Al-PFS/MoO_3).

An interesting interpretation from figure 3.2 and Table 3.1 is that the acid coating may be tailored to sensitize or de-sensitize the energetic composite. In the case of PFTD, the coating appears to enhance ignition sensitivity by

(i). reducing the onset of the PIR,

(ii). having lower activation energy; and,

(iii). promoting higher flame speeds.

The PFTD has a longer -CF_2- chain compared to PFS (figure 3.1). Longer chains are less stable and faster to react because they more readily form radicals compared to acids with smaller chains (T. W. Graham Solomons 2011). Also, PFTD contains higher fluorine wt. % (72% compared to 62% in PFS), which is a highly electronegative oxidizer. Dean et al. (Pantoya and Dean 2009) showed that the Al-F PIR is directly correlated with fluorine concentration and the specific surface area of the Al particle. Higher fluorine concentrations and specific surface areas lead to a lower PIR onset. This is also seen in figure 3.5 with a 30 °C reduction in onset PIR with PFTD compared with PFS. Reducing the onset for the PIR may accelerate the Al oxidation and explain the observation of increased burn velocity of Al-PFTD/MoO_3 compared to Al-PFS/MoO_3. Controlling the PIR onset may be a key to controlling the reactivity of the acid coated Al energetic composite.

Furthermore, PFS is a more symmetrically stable molecule compared to PFTD. Therefore, bond breaking and radical formation from PFS requires more energy than PFTD resulting in higher E_a. Also, oxygen and hydrogen from PFS carboxylic group may bond with fluorine radicals at the reaction front, further decreasing the concentration of fluorine available, consequently inhibiting Al oxidation and decreasing the burn velocity of the Al-PFS/MoO_3. Also, PFS molecules have an extra carboxylic acid functional group, consisting of

a π bond between carbon and oxygen. Although the -C-F- is one of the strongest single bonds with a bond dissociation energy (BDE) of 490 kJ/mol, the -C=O- is a π bond with a higher BDE of about 799-802 kJ/mol (T. W. Graham Solomons 2011). This means that almost twice the amount of energy required to cleave a -C-F- bond is necessary to cleave a -C=O- bond, which may also account for the higher E_a of Al-PFS/MoO_3. Thadani et al. (N. Thadhani 1999) showed that for solid state reactants, a reduced onset temperature would imply a higher reaction rate. It is very interesting to note that results from this study are consistent with Thadani et al. such that the onset temperature for Al-PFTD/MoO_3 is lower than Al-PFS/MoO_3 and the burn velocity and E_a are similarly correlated.

The burn velocity and E_a have an inverse relationship for the three energetic composites (Table 3.1). Activation energy measured here is apparent activation energy because the measurement considers influences beyond fuel-to-oxidizer ratio. The apparent activation energy quantifies the energy barrier needed to be overcome in order for a chemical reaction to occur. Reactants having high activation energy require greater energy input compared to reactants with lower activation energy.

Combustion of an energetic composite in a flame tube proceeds along the lateral axis of the flame tube. Given that the diameter of the flame tube (i.e., 3 mm) is smaller than its length (i.e., 10 cm) by an order of magnitude, heat transfer during the reaction may be approximated as one dimensional along the axis of propagation. Thermal stimulus via Nichrome wire heats up the portion of energetic composite in its vicinity, increasing the energy of the reactants above their activation energy. An exothermic reaction starts during the oxidation of the fuel. Energy released during this oxidation reaction heats the energetic composite adjacent to the reaction zone. Once the adjacent reactants obtain energy greater than its activation energy, the fuel and oxidizer particles start reacting exothermally. Thus, the reaction propagates in a flame tube. This progression of the reaction manifests itself as a fast moving flame front that can be observed visually. Energetic composites with low activation energy require comparatively less energy to overcome the E_a barrier. This implies that energy is more readily transferred to (rather than consumed by) unreacted energetic composite and the result is faster propagation of the reaction and higher burn velocity. On the other hand, energetic composites with comparatively higher E_a consume more energy at

the reaction site and result in lower burn velocity. This is exactly mirrored in the results as can be seen from Table 3.1.

4.0 CONCLUSIONS

The analysis of an approach to particle synthesis by functionalizing aluminum fuel particles lead to characterizations of reaction kinetics and combustion performance of aluminum-fluoropolymer reactions. Experiments were performed to alter key parameters of the reaction, namely flame speeds. Results show that enhanced outcome control and reaction tailorability may be achieved by simply altering the additive components.

Nanoscale aluminum particles were functionalized using perfluoro tetradecanoic acid (PFTD) bonded to the alumina passivation shell around Al. Three different energetic composites were created using molybdenum trioxide: Al functionalized with PFTD and MoO_3; non-functionalized Al with MoO_3 and individual PFTD particles; and non-functionalized Al with MoO_3 alone. Their flame speeds were measured in order to understand the effects of surface functionalization on aluminum reactivity. Results show that the surface functionalized Al composite (Al-PFTD/MoO_3) has a reaction rate twice that of Al/MoO_3 and three and a half times of Al/MoO_3/PFTD. The drastic change in the flame propagation and burn velocity was attributed to the proximity of the PFTD to the Al particles and hence, enhanced reaction kinetics.

Functionalization was further explored to tailor reactivity. Thermal equilibrium and flame propagation experiments were performed of three energetic composites each containing 80 nm average diameter Al particles combined with MoO_3, but two energetic composites contained Al coated particles with different acids and an uncoated Al energetic composite was used as a baseline for comparison. The acids were self-assembled monolayers of perfluorotetradecanoic acid (PFTD) and perfluoro sebacic acid (PFS) such that the energetic composites were labeled: Al-PFTD/MoO_3, Al-PFS/MoO_3 and Al/MoO_3. Results showed that Al-PFTD/MoO_3 had the highest velocity and almost double that of Al/MoO_3. On the other hand, Al-PFS/MoO_3 had the lowest velocity and 48% of Al/MoO_3. Equilibrium analyses revealed that the PFTD promoted a lower onset for a pre-ignition reaction which may be spurred by reduced structural stability of the acid molecular chain. The lower onset

for the fluorine aluminum pre-ignition reaction was the only difference in the heat flow trends for the two different acid coatings and may be an indication of the key to increasing or decreasing the reactivity of the acid coated Al energetic composites.

Activation energy (E_a) showed a completely inverse trend with velocity, with highest velocity associated with the lowest E_a. This finding was anticipated because propagation velocity can be described as a series of ignition sites such that lower activation energy correlates with higher propagation velocity for the similar energetic composites examined here.

These findings are impactful because they suggest that the structure of the acid coating can be tailored to enhance or reduce the reactivity of the energetic composite. Results suggest that because the perfluorotetradecanoic acid (PFTD) coating is less stable and contains a higher concentration of fluorine, these factors promote an earlier onset of a pre ignition reaction that enhances energetic composite reactivity (results in higher velocity and lower activation energy). On the other hand, perfluoro sebacic acid (PFS) is more stable, requires greater bond energy for dissociation and results in a delayed onset for the PIR, higher activation energy and lower flame speeds; reducing the overall energetic composite reactivity.

4. Acknowledgements

The authors are grateful for support from the Army Research Office (W911NF-11-10439 and W911NF-14-10250) and encouragement from our program manager, Dr. Ralph Anthenien.

REFERENCES

Aumann, C., G. Skofronick, and J. Martin. "Oxidation behavior of aluminum nanopawders." *Journal of Vacuum Science and Technology* 13, no. 3 (1995): 1178-1183.

B. Dickiki, S. Dean, M. Pantpya, V. Levitas, J. Jouet. "Influence of aluminum passivation on reaction mechanism: flame propagation studies." *Energy & Fuels* 23 (2009): 4231-4235.

B. S. Bockmon, M. L. Pantoya, S. F. Son, B. W. Asay, J. T. Mang. "Combustion velocities and propagation mechanisms of metastable interstitial composites." *Journal of Applied Physics* 98, no. 6 (2005): 064903-7.

Bockmon, B., M. Pantoya, S. Son, B. Asay, and J. Wang. "Combustion wavespeeds and propagation mechanisms of metastable interstitial composites." *Propellants, Explosives, Pyrotechnics* 98, no. 6 (2005): 1-7.

Brown, M., S. Taylor, and M. Tribelhom. "Fuel oxidant particle contact in binary pyrotechnic reactions." *Propellants Explosives Pyrotechnics* 23 (1998): 320-327.

C. Crouse, C. Pierce, J. Spowart. "Influencing solvent miscibility and aqueous stability of aluminum nanoparticles through surface functionalization with acrylic monomers." *ACS Applied Materials and Interfaces* 2 (2010): 2560-2569.

C. Yarrington, S. Son, T. Foley, S. Obrey, A. Pacheo. "Nano aluminum energetics: the effect of synthesis method on morphology and combustion performance." *Propellants, Explosives, Pyrotechnics* 36, no. 6 (2011): 551-557.

Clayton, N., K. Kappagantula, M. Pantoya, S. Kettwich, and S. Iacono. "Fabrication, characterization and energetic properties of metalized fibers." *ACS Applied Materials and Interfaces* Article ASAP (2013).

CRC Handbook of Chemistry and Physics. 71. Boca Raton, FL: CRC Press, 1991.

Cudzilo, S., M. Szala, A. Huczko, and M. Bystrzejewski. "Combustion reactions of poly carbon monofluoride with different reductants and characterization of the products." *Propellants, Explosives, Pyrotechnics* 32, no. 2 (2007): 149-154.

D. Osborne, M. Pantoya. "Effect of Al particle size on the thermal degradation of Al/Teflon mixtures." *Combustion Science and Technology* 179, no. 8 (2007): 1467-1480.

D. Pesiri, C. Aumann, L. Bilger, D. Booth, R. Carpenter, R. Dye, E. O'Neill, D. Shelton, K. Walter. "Industrial scale nano aluminum powder manufacturing." *Journal of Pyrotechnics* 19 (2004): 19-32.

D. Stamatis, E. L. Dreizen, K. Higa. "Thermal initiation of al-MoO3 nanocomposite materials prepared by different methods." *Journal of Propulsion and Power* 27 (2011): 1079-1087.

D. Weibel, A. Michels, A. Feil, L. Amaral, S. Teixeria, F. Horowitz. "Adjustable hydrophobicity of Al substrates by chemical surface functionalization of nano/microstructures." *The Journal of Physical Chemistry C*, 2010: 13219-13224.

Danielson, S., et al. "Metastable metalized perfluoropolyether functionalized composites." *American Chemical Society.* New Orleans, LA, 2013.

Dreizin, E. "Metal based nanoreactive materials: A review article." *Progress in Energy and Combustion Science* 35, no. 2 (2009): 141-167.

Fantasia, R., S. Pierson, C. Hawkins, S. Iacono, and S. Kettwich. "Facile route towards perfluoropolyether segmented polyurethanes." *American Chemical Society.* Denver, CO, 2011.

Farley, Cory. "Reactions of Aluminum with Halogen Containing Oxides." *Dissertation.* Lubbock, TX, May 2013.

Gesner, Jeff, Michelle Pantoya, and Valery Levitas. "Effect of oxide shell growth on ano-aluminum thermite propagation rates." *Combustion and Flame* 159 (2012): 3448-3453.

I. Liakosa, E. McAlpineb, X. Chen, R. Newmand, M. R. Alexander. "Assembly of octadecyl phosphonic acid on the α-Al2O3 (0 0 0 1) surface of air annealed alumina: Evidence for termination dependent adsorption." *Applied Surface Science* 255, no. 5 (2008): 3276-3282.

J. Brege, C. Hamilton, C. Crouse, A. Barron. "Ultrasmall carbon nanoparticles from a hydrophobically immobilized surfactant template." *Nano Letters*, 2009: 2239-2242.

J. Folkers, C. Gorman, P. Laibinis, S. Buchholz, G. Whitesides, R. Nuzzo. "Self-assembled monolayers of long-chain hydroxamic acids on the native oxide of metals." *Langmuir*, 1995: 813-824.

J. H. Bae, D. K. Kim, T. H. Jeong, H. J. Kim. "Crystallization of amorphous Si thin films by the reaction of MoO3/Al." *Thin Solid Films* 518 (2010): 6205-6209.

J. Horn, J. Lightstone, J. Carney, J. Jouet. "Preparation and characterization of functionalized aluminum nanoparticles." *SHOCK COMPRESSION OF CONDENSED MATTER - 2011: Proceedings of the Conference of the American Physical Society Topical Group on Shock Compression of Condensed Matter.* Chicago, Illinois, 2011.

J. Sun, M. Pantoya, S. Simona. "Dependence of size and size distribution on reactivity of aluminum." *Thermochimica Acta* 444 (2006): 117-127.

Johns, K., and G. Stead. "Fluoroproducts - the extremophiles." *Journal of Fluorine Chemistry* 104 (2000): 5-14.

K. Oberg, P. Persson, A. Shchukarev, B. Eliasson. "Comparison of monolayer films of stearicacid and methyl stearate on an." *Thin Solid Films* 397 (2001): 102-108.

K. Wefers, C. Misa. "Oxides and hydroxides of aluminum." *Alcoa Technical Paper* 19 (1988).

Kappagantula, K., and M. Pantoya. "Experimentally measured themal transport properties of aluminum-polytetrafluoroethylene nanocomposites with graphene and carbon nanotube additives." *International Journal of Heat and Mass Transfer* 55, no. 4 (2012): 817-824.

Kappagantula, K., B. Clark, M. Pantoya, and Keerti Kappagantula. "Flame propagation experiments of non gas generating nanocomposite reactive materials." *Energy & Fuels* 25, no. 2 (2011): 640-646.

Kappagantula, K., C. Farley, M. Pantoya, and J. Horn. "Tuning energetic material reactivity using surface functionalization of aluminum fuels." *The Journal of Physical Chemistry C* 116, no. 46 (2012): 24469-24475.

Kappagantula, K., M. Pantoya, and Hunt E. "Impact ignition of aluminim-teflon based energetic materials impregnated with nano-structured carbon additives." *Journal of Applied Physics* 112, no. 2 (n.d.): 024902-024908.

Kappagantula, K., M. Pantoya, and J. Horn. "Effect of surface coatings on aluminum fuel particles toward nanocomposite combustion." *Surface and Coatings Technology* 237 (2013): 456-459.

Kettwich, S., K. Kappagantula, B. Kusel, E. Avijan, and S. Danielson. "Thermal investigations of nanoaluminum/perfluoropolyether core-shell impregnated composites for structural energetics." *Thermochimica Acta* 591 (2014): 45-50.

Kirsch, P. *Modern Fluoroorganic Chemistry: Synthesis, REactivity, Applications.* Hoboken, NJ: John Wiley and Sons, 2004.

Koch, E. "Metal-fluorocarbon pyrolants IV: Thermochemical and combustion behavior od magnesium/teflon/viton (MTV)." *Propellants, Explosives, Pyrotechnics* 27, no. 6 (2002): 340-351.

Koch, E. "Metal-fluorocarbon pyrolants: III. Development and application of magnesium/teflon/viton (MTV)." *Propellants, Explosives, Pyrotechnics* 27, no. 5 (2002): 262-266.

Koch, E. "Metal-fluorocarbon pyrolants: V. Theoretical evaluation of the combustion performance of metal-fluorocarbon pyrolants based on strained fluorocarbons." *Propellants Explosives Pyrotechnics* 29, no. 1 (2004): 9-18.

M. Abela, J. Wattsa, R. Digby. "The adsorption of alkoxysilanes on oxidised aluminium substrates." *International Journal of Adhesion and Adhesives*, 1998: 179-192.

M. Lee, K. Feng, X. Chen, N. Wu, A. Raman, J. Nightingale, E. Gawalt, D. Korakakis, L. Hornak, A. Tiperman. "Adsorption and desorption of stearic acid on self-assembled monolayers on aluminum oxide ." *Langmuir*, 2007: 2444-2452.

M. Weismiller, J. Malchi, J. Lee, R. Yetter, T. Foley. "Effects of fuel and oxidizer particle dimensions on the propagation of aluminum containing thermites." *Proceedings of Combustion Institute* 33, no. 2 (2011): 1989-1996.

M.E. Karaman, D.A. Antelmi, R.M. Pashley. "The production of stable hydrophobic surfaces by the adsorption of hydrocarbon and fluorocarbon carboxylic acids onto alumina substrates." *Colloids and Surfaces A: Physicochemical and Engineering Aspects* 182, no. 1-3 (2001): 285-298.

McKeen, Laurence. *Fluorinated Coatings and Finishes Handbook:The Definitive Users Guide.* William Andrew, 2006.

Moldoveanu, S. *Analytical properties of synthetic organic polymers.* Amsterdam: Elsevier, 2005.

N. Thadhani, S. Namjoshi, K. Vandersall, X. Xu. *Thermal analysis instrumentation for the kinetics of shocked materials.* Final report, Atlanta: Storming Media, 1999.

Pantoya, M., and S. Dean. "The influence of alumina passivation on nano-Al/Teflon reactions." *Thermochimica Acta* 493 (2009): 109-110.

Pierson, S., D. Richard, C. Lindsay, S. Iacono, and S. Kettwich. "Synthesis and characterization of aluminum perfluoropolyether blended materials." *American Chemical Society.* Anaheim, CA, 2011.

Prentice, D., M. Pantoya, and B. Clapsaddle. "Effect of nanocomposite synthesison the combustion performance of a ternary thermite." *Journal of Physical Chemistry B* 109, no. 43 (2005): 20180-20185.

R. Brewer, P. Dixon, S. Ford, K. Higa, R. Jones. *Lead free electric primer.* Final, China Lake, CA: Naval Air Warfare Center, WEapoms Division, 2006.

R. J. Jouet, A. Warren, D. M. Rosenberg, V. J. Bellito, K. Park, M. Zachariah. "Surface passivation of bare aluminum nanopaticles using perfluoroalkyl carbozylic acids." *Chemistry of Materials* 17 (2005): 2987-2996.

R. Thiruvengadathan, A. Bezmelnitsyn, S. Apperson, C. Staley, P. Redner, W. Balas, S. Nicolich, D. Kapoor, K. Gangopadhyaya, S. Gangopadhyay. "Combustion characteristics of novel hybrid nanoenergetic formulations." *Combustion and Flame* 158 (2011): 964-978.

S. H. Fischer, M. C. Grubelich. "Theoretical energy release of thermites, intermetallics and combustible metals." *24th International Pyrotechnics Seminar.* Monterey, CA, 1998.

S. Nandagopal, M. Mehilal, M. Tapaswi, S. Jawalkar, K. Radhakrishnan, B. Bhattacharya. "Effect of coating of ammonium perchlorate with fluorocarbon on ballistic and sensitivity properties of AP/Al/HTPB." *Propellants, Explosives, Pyrotechnics* 34, no. 6 (2009): 526-531.

S. Valliappan, J. Swiatkiewicz, J.A. Puszynski. "Reactivity of aluminum nanopowders with metal oxides." *Powder Technology* 156 (2005): 164-169.

Shimizu, A., and J. Saitou. "Effect of contact points between particles on the reaction rate in the Fe2O3-W2O5 system." *Solid State Ionics* 38 (1990): 261-269.

Starnik, M. J. "Analysis of aluminum based alloys by calorimetry: quantitative analysis of reactions and reaction kinetics." *International Materials Review* 49, no. 3 (2004): 191-226.

T. W. Graham Solomons, C. Fryhle. *Organic Chemistry.* Wiley, 2011.

Turns, Stephen R. *An Introduction to Combustion: Concepts and Applications, Third Edition.* 3. New York: McGraw Hill, 2012.

Watson, K., M. Pantoya, and V. Levitas. "Fast reactions with nano- and micrometer aluminum: A study on oxidation versus fluorination." *Combustion and Flame* 155, no. 4 (2008): 619-634.

Yarrington, C., S. Son, and T. Foley. "Combustion of silicon/teflon/viton and aluminum/teflon/iton energetic composites." *Journal of Propulsion and Power* 26, no. 4 (2010): 734-743.

Yetter, R., G. Risha, and S. Son. "Metal combustion and nanotechnology." *Proceedings of Combustion Institute* 32, no. 2 (2009): 1819-1838.